35th Annual International Conference of the IEEE EMBS
Osaka, Japan, 3 - 7 July, 2013

QRS classification and spatial combination for robust heart rate detection in low-quality fetal ECG recordings

G. Warmerdam, R. Vullings, C. Van Pul, P. Andriessen, S.G. Oei, P. Wijn

Abstract— **Non-invasive fetal electrocardiography (ECG) can be used for prolonged monitoring of the fetal heart rate (FHR). However, the signal-to-noise-ratio (SNR) of non-invasive ECG recordings is often insufficient for reliable detection of the FHR. To overcome this problem, source separation techniques can be used to enhance the fetal ECG. This study uses a physiology-based source separation (PBSS) technique that has already been demonstrated to outperform widely used blind source separation techniques. Despite the relatively good performance of PBSS in enhancing the fetal ECG, PBSS is still susceptible to artifacts. In this study an augmented PBSS technique is developed to reduce the influence of artifacts. The performance of the developed method is compared to PBSS on multi-channel non-invasive fetal ECG recordings. Based on this comparison, the developed method is shown to outperform PBSS for the enhancement of the fetal ECG.**

I. Introduction

In obstetric units, timely recognition of fetal distress is a great challenge. At present, cardiotocography (CTG) is the most widespread method for fetal monitoring. Unfortunately, CTG has a poor specificity, making its diagnostic value limited [1]. Besides, to detect the fetal heart rate (FHR), CTG uses Doppler ultrasound, which is sensitive to movement and transmits energy into the fetal body. As an alternative, non-invasive fetal electrocardiography (fECG), obtained from electrodes attached to the maternal abdomen, might provide a more robust and safer technique for prolonged monitoring of the FHR.

The non-invasive fECG recordings are strongly contaminated by unwanted electrical interferences. In addition, the low amplitude of the fECG with respect to the amplitude of these interferences makes the detection of the FHR difficult. Of all interferences in the abdominal recordings, the dominant interference is the maternal ECG (mECG). In the literature, several techniques have been proposed for suppression of the mECG, as briefly summarized in [2]. The abdominal signals remaining after mECG suppression still contain other interferences and their signal-to-noise-ratio (SNR) is often insufficient for robust detection of the FHR. To enable detection of the FHR, additional signal processing steps are required.

In a simplified model, the electrical activity of the heart can be represented by a single electrical field vector that varies in amplitude and orientation over time, called the (three dimensional, 3D) vectorcardiogram (VCG) [3]. In this model, each ECG lead consists of a linear combination of the three components of the VCG. The measured fetal ECG at the maternal abdomen (with $N > 3$ lead signals) contains common components of the fECG and is, therefore, spatially correlated.

Several techniques have been proposed to exploit this spatial correlation to enhance the SNR of the fECG [4], [5], [6]. Of these techniques, [4], [5] are so called blind source separation (BSS) techniques, that require no a priori knowledge of the physiology of the fetal cardiac electrical system. However, this lack of physiological basis reduces the efficiency of the BSS techniques to separate the fECG from the noise in case of low SNR [6], as is typical for non-invasive fECG recordings.

As an alternative to the BSS techniques, Vullings et al. proposed a physiology-based source separation (PBSS) technique [6]. The PBSS technique spatially combines the abdominal fECG signals, based on knowledge of the positions of the recording electrodes, to obtain the VCG. The VCG has maximum amplitude during ventricular depolarization and the direction in which the VCG has maximum amplitude is referred to as the electrical axis of the heart. Projection of the VCG onto this axis maximizes the amplitude of the QRS complex, the part of the fECG that is associated with ventricular depolarization. These QRS complexes need to be detected to obtain the FHR.

Whereas the ability of BSS techniques to extract the fECG depends on the SNR, the use of a priori knowledge in PBSS allows to linearly combine (and enhance) the fECG regardless of the SNR. Although PBSS has been demonstrated to outperform BSS techniques, especially for recordings with low SNR [6], PBSS is susceptible to artifacts. In this study an augmented physiology-based source separation technique (PBSSa) is developed that reduces the influence of artifacts in the enhancement of the fECG.

II. Fetal ECG enhancement

A flowchart of the signal processing steps used in PBSS and PBSSa to enhance the fECG, is shown in Fig. 1. In both techniques, the signals of the individual leads remaining after mECG suppression ($\mathbf{V}$) are combined into the VCG ($\mathbf{S}$) by a fixed linear combination [7]. Since the typical time-path of the QRS loop in the VCG through 3D space has a planar shape [8] and resembles an ellipse, an ellipse fit is used to determine the direction of the electrical axis. The electrical axis is approximated by the elliptic long axis ($\vec{r}_{long}$). Prior to the ellipse fit, a sample selection attempts to primarily include those samples (j) of the VCG in the ellipse fit, that

G. Warmerdam and R.Vullings are with the Faculty of Electrical Engineering, Eindhoven University of Technology, Eindhoven, The Netherlands g.j.j.warmerdam@tue.nl

C.Van Pul, P. Andriessen, S.G. Oei, and P. Wijn are with the Máxima Medical Centre, Veldhoven, The Netherlands

978-1-4577-0216-7/13/$26.00 ©2013 IEEE

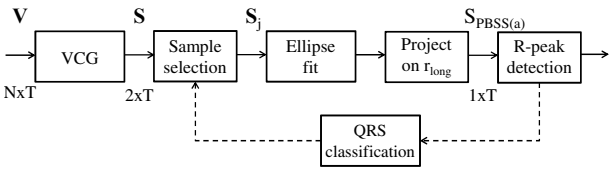

Fig. 1. Flow chart of the signal processing sequence to enhance the fECG, with **V** the signals remaining after mECG suppression, N is the number of lead signals, and T the sample length of the VCG.

contain information of the QRS complexes. The selected data for the ellipse fit are further denoted as $\mathbf{S}_j$. Then, **S** is projected onto $\vec{r}_{long}$ to obtain a fECG with enhanced QRS complexes. The projected signal is further denoted as S_{PBSS} and S_{PBSSa} for PBSS and PBSSa, respectively. Subsequently, a wavelet-based R-peak detection is performed in $S_{PBSS(a)}$ to detect the FHR [9].

Note that to account for changes in the orientation of the electrical axis due to fetal movement, PBSS calculates the orientation of $\vec{r}_{long}$ based on the ellipse fitted to $\mathbf{S}_j$ in a moving window of 10 seconds length. After each step (n), the window is shifted by two seconds. Furthermore, this study uses a 2D representation of the VCG (in the coronal plane) because the 2D VCG is less susceptible to artifacts than the 3D VCG and because the third dimension of the 3D VCG (sagittal plane) is often difficult to estimate from the non-invasive fECG recordings.

In the original PBSS technique, interferences in **V** other than the mECG are partly suppressed by frequency selective filtering. Taking into account the frequency content of the fetal ECG [10], the signals are filtered by a fourth order Butterworth high-pass and low-pass filter with cutoff frequency of 15 Hz and 35 Hz, respectively. However, despite the high- and low-pas filtering, a significant fraction of these interferences remains.

Correct estimation of the electrical axis is crucial since inaccuracies in the direction of this axis directly affect the quality of the QRS complexes in $S_{PBSS(a)}$. The main limitation of PBSS is that the estimation of the electrical axis is susceptible to artifact. To reduce the influence of artifacts in the ellipse fit, that is used to estimate the electrical axis, this study presents an improved sample selection in combination with a newly developed QRS classification (indicated by the dotted line in Fig. 1). To further increase the robustness of the electrical axis estimation, an assessment is performed on the orientation of the estimated electrical axis. These improvements are discussed in detail in Section II-A, II-B, and II-C.

A. Sample selection

In the estimation of the electrical axis by PBSS, the noise is assumed to be limited to the lower 90% of the VCG amplitudes. These amplitudes are determined as the Euclidian distance from the origin. Artifacts with amplitude larger than the QRS complex are assumed to occur less than 1% of the time. For these reasons, only the top 10% of the samples of the VCG is retained and the upper 1% is omitted. If either one of these assumptions is false, e.g. due to a relatively large noise amplitude in the VCG or the presence of numerous artifacts, the ellipse fit will be affected and the estimation of the electrical axis will be inaccurate. As a result, the SNR of the QRS complexes in S_{PBSS} will decrease.

In contrast to PBSS, sample selection for the ellipse fit in PBSSa is based on previously detected QRS complexes. PBSSa only includes samples provided by m previously located QRS complexes that were identified by the R-peak detection. This sample selection ensures that only the information of QRS complexes is used to estimate the electrical axis and that no selection based on the VCG amplitude is required, as shown in Fig. 2.

The choice for m QRS complexes to produce the VCG ensures that the influence of a detected artifact that is accidentally detected as QRS complex (mis-detection) is reduced. On the other hand, fetal movement can change the orientation of the electrical axis and information from previously detected QRS complexes might be outdated. Therefore, the value of m is a trade-off between robustness against mis-detections and the ability to account for changes in the orientation of the electrical axis due to fetal movement, and is experimentally determined as 10.

B. QRS classification

Before a QRS complex Z_i is included in the data used for the ellipse fit ($\mathbf{S}_j$), it is analyzed by comparing the QRS waveform and energy content to a running average of the QRS waveform ($\bar{Z}$) to verify that Z_i is not a mis-detection. If a QRS complex is classified as a mis-detection, Z_i is not included in $\mathbf{S}_j$.

The QRS complex Z_i is defined by a 50ms window centered around the i^{th} R-peak and baseline fluctuations in Z_i are suppressed by a fourth order Butterworth high-pass filter with a cutoff frequency of 1.5 Hz. The resemblance in QRS waveform between Z_i and $\bar{Z}$ is evaluated by means of the inproduct between the normalized Z_i and the normalized $\bar{Z}$ (further denoted as $\hat{Z}_i$ and $\hat{\bar{Z}}$, respectively). The energy of the waveforms is determined as the variance in the (unnormalized) QRS complexes Z_i and $\bar{Z}$.

The minimally required inproduct between $\hat{Z}_i$ and $\hat{\bar{Z}}$ is denoted as C_I, and the maximally allowed energy difference between Z_i and $\bar{Z}$ as C_E. The values of C_I and C_E are empirically determined as 0.95 and 3 respectively. If the inproduct between $\hat{Z}_i$ and $\hat{\bar{Z}}$ is less than C_I, or the energy of Z_i is either larger than C_E or smaller than $\frac{1}{C_E}$ times the energy of $\bar{Z}$, the complex Z_i is not included in the ellipse fit.

C. Assessment of the estimated electrical axis

Besides fetal movement, also artifacts in the VCG can cause changes in the estimated orientation ($\vec{r}_{long}$) of the electrical axis that are unrelated to changes due to fetal movement. In PBSS, the estimation of the electrical axis cannot distinguish between changes in orientation of the axis due to fetal movement or due to artifacts. However, changes due to fetal movement are typically gradual, whereas changes due to artifacts can be arbitrarily large. As a result, the

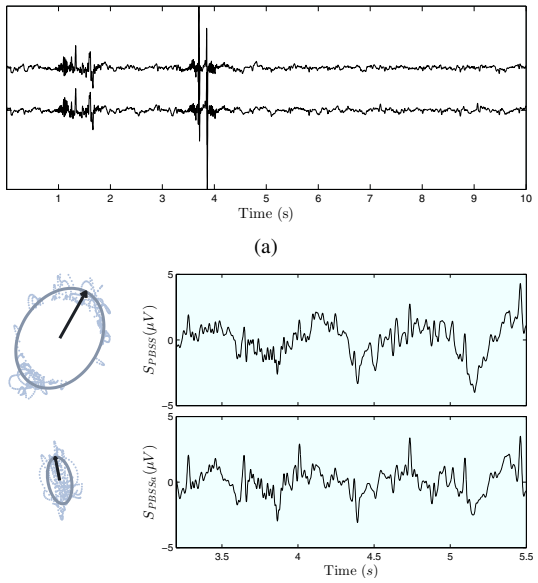

Fig. 2. Effect of an artifact on the estimation of the electrical axis for PBSS and PBSSa. (a) Two out of eight signals of **V** are displayed with artifacts disturbing the abdominal fECG around 1.5 and 4 seconds. (b) The left images display the ellipse fit for PBSS (above) and PBSSa (below). The points correspond to $\mathbf{S}_j$ and the arrow corresponds to $\vec{r}_{long}$. The difference in amplitude of the VCG of PBSS compared to PBSSa is caused by the artifact in **V**. The presence of the artifact does not disturb the VCG of the PBSSa. The angle between the estimated electrical axis of PBSS and PBSSa is 40°. The right graphs display S_{PBSS} (above) and S_{PBSSa} (below). The combined effect of improved sample selection, QRS classification, and assessment on the orientation of $\vec{r}_{long}$, results in improved quality of the QRS complexes in S_{PBSSa} with respect to the QRS complexes in S_{PBSS}.

orientation of $\vec{r}_{long}$ in PBSS is not necessarily related to the actual electrical axis in the case that an artifact disturbs the ellipse fit. This can lead to a reduced quality of the QRS complexes in S_{PBSS}.

To distinguish changes in the orientation of $\vec{r}_{long}$ caused by fetal movement from changes caused by artifacts, a new orientation ($\vec{r}_{long}[n+1]$) is restricted with respect to a previous orientation ($\vec{r}_{long}[n]$). Instead of accepting the new orientation $\vec{r}_{long}[n+1]$, the orientation change in $\vec{r}_{long}$ is restricted by means of a learning rate C_{LR}. The orientation of the new projection axis is given by

$$\hat{\vec{r}}_{long}[n+1] = \mathbf{R}(C_{LR} \cdot \theta)\hat{\vec{r}}_{long}[n] \qquad (1)$$

with $\mathbf{R}(x)$ the (2D) rotation-matrix over x radians. In Eq. (1), θ describes the angle between the previously calculated $\hat{\vec{r}}_{long}[n]$ and a newly found $\vec{r}_{long}[n+1]$. The use of C_{LR} ensures that the projection axis only fully adjusts to a new orientation if this orientation lasts for several steps. The value of C_{LR} is a trade-off between sensitivity to fetal movement and robustness against artifacts, and is chosen $\frac{1}{3}$.

D. Implementation

Due to the fact that PBSSa requires knowledge on locations of QRS complexes, PBSSa is only activated after sufficient QRS complexes have been detected and classified as correct in an initialization phase. Furthermore, if no QRS complex is identified for a prolonged period of time, fetal movement could have occurred in between. The information contained by these previously detected QRS complexes about the orientation of the electrical axis might be outdated. Therefore, if any of the QRS complexes used for the estimation of the electrical axis is older than 10 seconds, the traditional PBSS is used as source separation technique.

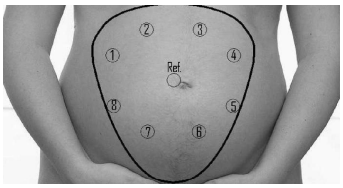

Fig. 3. Schematic illustration of the electrode configuration on the maternal abdomen. The ground electrode is not displayed.

Since no a priori information is available about an average QRS waveform, QRS classification in the initialization phase is based on the R-R intervals of consecutive R-peaks, rather than on QRS waveform. The initialization phase searches for m consecutive peaks for which all individual R-R intervals are within the physiological R-R boundaries (based on a heart rate of 50-255 BPM in accordance with the values used in [9]) and no R-R interval deviates more than 20% from the average R-R value. After m QRS complexes have been identified and accepted, PBSSa is used for further signal processing.

III. Evaluation

A. Data acquisition

For this study, an in-house database is used to evaluate the performance of the developed algorithms. In total, recordings have been performed in 13 women after having given written informed consent, with gestational age ranging from 22 to 41 weeks. The recordings are 200 seconds long, consisting of 8 bipolar signals with the electrode configuration as schematically illustrated in Fig. 3. The measurements are performed at the Máxima Medical center (Veldhoven, the Netherlands) and are acquired at a sample frequency of 1 kHz. The recordings are preprocessed to suppress the mECG by an adaptive template-based technique [2] and the fetal VCG is obtained by a vectorcardiography method [7].

B. Evaluation criteria

To compare the performance of PBSSa and PBSS, visual annotation is used as a gold standard. This annotation is performed by an expert, in the signals that remain after suppression of the mECG (**V**). Evaluation criteria used to quantify the performance of the developed algorithm are based on the percentage of correctly detected QRS complexes and the SNR.

The percentage of correctly detected QRS complexes is expressed by means of the sensitivity (Se) and the positive predictive value (PPV):

$$Se = \frac{nTP}{nTP+nFN} \cdot 100\% \qquad (2)$$

$$PPV = \frac{nTP}{nTP+nFP} \cdot 100\% \qquad (3)$$

TABLE I

PERFORMANCE OF PBSSA COMPARED TO PBSS, BASED ON SE, PPV, AND THE SNR.

Technique	SNR (dB, median)	$Se(\%)$	$PPV(\%)$
PBSS	11.7	93.9	97.7
PBSSa	**12.7**	**95.3**	**97.7**

with nTP the number of True Positives (correctly detected peaks), nFP the number of False Positives (falsely detected peaks), and nFN the number of False Negatives (missed peaks). The Se and PPV are calculated based on the total nTP, nFP and nFN found in all 13 recordings.

Besides based on the percentage of correctly detected QRS complexes, improvements in the signal enhancement can also be quantified based on the SNR. Confer with the definition of SNR in [6], the SNR is measured by comparing a running average QRS complex $\hat{\bar{Z}}$ in $S_{PBSS(a)}$ to the individual QRS complexes $\hat{Z}_i$ in $S_{PBSS(a)}$. The SNR ($\Psi_{SNR,i}$) of Z_i is calculated as

$$\Psi_{SNR,i}(dB) = 10\log\frac{\hat{Z}_{ave}\cdot\hat{Z}_{ave}^{T}}{(\hat{Z}_i-\hat{Z}_{ave})(\hat{Z}_i-\hat{Z}_{ave})^{T}} \qquad (4)$$

IV. RESULTS

In PBSSa, the original PBSS technique is used in 1% of the recording time. The performance measures for PBSS (for the entire database) and PBSSa are shown in Table I. The median of the SNR for PBSSa measures 12.7dB, compared to 11.7dB for PBSS. For PBSSa the Se is 1.5% higher than for PBSS (95.3% versus 93.9%, respectively). The PPV for PBSSa and PBSS is similar (97.7% versus 97.7%, respectively).

V. DISCUSSION & CONCLUSIONS

In this study, a physiology-based technique is used for source separation of fECG recordings [6]. The main limitation of the existing PBSS is the susceptibility to artifacts in the estimation of the electrical axis. In PBSS, correct estimation of the electrical axis is directly related to the quality of the QRS complexes in the resulting fECG signal after source separation. Hence, improvements that are developed in this study mainly aim to provide a more robust estimation of the electrical axis.

The developed sample selection and QRS classification to improve the ellipse fit, allow for improved estimation of the electrical axis, even in case the VCG is contaminated with artifacts. Besides, PBSSa assesses the change in orientation of the estimated electrical axis with regard to physiologically acceptable fetal movement.

In [6] it is already shown that PBSS outperforms other widely used blind source separation techniques, such as independent component analysis [5], in particular for the non-invasive fECG recordings that exhibit a low SNR. Therefore, this study only compares the performance of the developed PBSSa algorithm to the original PBSS technique.

The performance of PBSS and PBSSa is evaluated by means of the SNR of the enhanced fECG, and the Se and PPV of the detected FHR. Whereas the SNR indicates improvement in the quality of the QRS complexes after source separation, the Se and PPV directly reflect the actual improvement in the detection of QRS complexes.

Based on the increase in the SNR (from 11.7dB to 12.7dB for PBSS and PBSSa, respectively), it can be concluded that the estimation of the electrical axis has improved for PBSSa with respect to PBSS. In particular in the vicinity of artifacts, the improved estimation of the electrical axis in PBSSa leads to a decrease in the number of missed peaks. As a result, the Se increases for PBSSa compared with the Se for PBSS (from 93.9% to 95.3%). Since artifacts only occur infrequently in the used database, the decrease in the number of missed peaks is relatively small compared with the total number of annotated peaks. However, these infrequent disturbances in the FHR might have a significant influence on a consecutive analysis of the FHR, e.g. by spectral analysis [11]. Unlike the decrease in the number of missed peaks, the number of falsely detected peaks is similar for PBSS and PBSSa, resulting in a similar PPV (97.7%). The similar number of falsely detected peaks for both techniques is because the same peak detection algorithm [9] is used in PBSS and PBSSa.

The combined effect of the developed QRS classification to select QRS samples and the assessment of the orientation of the estimated electrical axis has led to a reduction of the influence of artifacts in PBSSa. The increased SNR in PBSS allows for improved detection of the FHR, as evidenced by the increase in Se, with respect to PBSS.

REFERENCES

[1] Z. Alfirevic, D. Devane, and G M L. Gyte. Continuous cardiotocography (CTG) as a form of electronic fetal monitoring (EFM) for fetal assessment during labour. *Cochrane Database Syst Rev*, (3):CD006066, 2006.

[2] R. Vullings, C.H.L. Peters, R.J. Sluijter, M. Mischi, S.G. Oei, and J.W.M. Bergmans. Dynamic segmentation and linear prediction for maternal ECG removal in antenatal abdominal recordings. *Physiol Meas*, 30(3):291–307, Mar 2009.

[3] E. Frank. General theory of heat-vector projection. *Circ Res*, 2(3):258–270, May 1954.

[4] E.C. Karvounis, M.G. Tsipouras, and D.I. Fotiadis. Detection of fetal heart rate through 3-D phase space analysis from multivariate abdominal recordings. *IEEE Trans Biomed Eng*, 56(5):1394–406, May 2009.

[5] S. Waldert, M. Bensch, M. Bogdan, W. Rosenstiel, B. Schölkopf, C.L. Lowery, H. Eswaran, and H. Preissl. Real-time fetal heart monitoring in biomagnetic measurements using adaptive real-time ICA. *IEEE Trans Biomed Eng*, 54(10):1867–1874, Oct 2007.

[6] R. Vullings, C.H.L. Peters, M.J.M. Hermans, P.F.F. Wijn, S.G. Oei, and J.W.M. Bergmans. A robust physiology-based source separation method for QRS detection in low amplitude fetal ECG recordings. *Physiol Meas*, 31(7):935–951, Jul 2010.

[7] G.E. Dower, H.B. Machada, and J.A. Osborne. On deriving the electrocardiogram from vectorcardiographic leads. *Clin Cardiol*, 3:87–95, 1980.

[8] F. Shellong. *Grundzüge einer klinischen Vektocardiographie des Herzens*. Springer-Verlag, Berlin, 1939.

[9] M.J. Rooijakkers, C. Rabotti, S.G. Oei, and M. Mischi. Low-complexity R-peak detection for ambulatory fetal monitoring. *Physiol Meas*, 33(7):1135–1150, Jul 2012.

[10] S. Abboud and D. Sadeh. Spectral analysis of the fetal electrocardiogram. *Comput Biol Med.*, 19(6):409–415, 1989.

[11] C.H.L. Peters, R. Vullings, M.J. Rooijakkers, J.W.M. Bergmans, S.G. Oei, and P.F.F. Wijn. A continuous wavelet transform-based method for time-frequency analysis of artefact-corrected heart rate variability data. *Physiol Meas*, 32(10):1517–1527, Oct 2011.